Digging mechanics and path selection in *Zophobas morio* larvae

Andy Cohen, Jason Doyle

December 14, 2016

Abstract

Many animals' locomotion have been extensively studied, but the mechanism by which beetle larvae dig has been poorly studied. We explore the mechanisms by which *Zophobas morio* larvae dig through granular media and how they select a path by which to progress through the medium. We found that, contrary to predictions based on frictional energy losses, the larvae chose steep angles of attack that increased linearly as the friction angle of the medium increased. We also developed image processing algorithms for collecting state variables of the larva and surrounding granular medium particles over the course of a video. These states will be used as the inputs in a discrete element model that will further explore our preliminary results and test our hypothesis that the larvae choose paths to minimize their energy costs.

1 Introduction

Many beetle larvae dig in granular media such as soil. Tiger beetle larvae do so to ambush prey, Japanese beetle larvae dig to feed on roots, and the *Zophobas morio* larvae studied in this paper dig to evade predators. Digging behavior has been studied before [1], but only in behavioral terms-the mechanism by which this behavior occurs has not yet been studied. Other animals' distinct mechanisms of locomoting through granular media have also been studied: the Razor clam's method of burrowing [2], [3] and the sandfish's method of undulating through the sand [4] have been previously explained. We thus attempt to similarly explain the mechanism by which beetle larvae dig.

When moving, many animals prefer one gait or mode of locomotion over others in order to keep their power consumption at a constant value [5]. Constant power P for a larva can be defined as the total energy E required to submerge the larva's body in the medium divided by the total time t to do so, as given by $P = \frac{E}{t}$ [6]. Given a fixed power, it is thus necessary to decrease E in order to also decrease the time t it takes a larva to bury itself. Energy costs of locomotion also exert a selective pressure on animals-those with lower costs are less likely to die from starvation and better able to redirect energy to other advantageous tasks such as enhanced sensory processing [7]. Those that have survived are likely to have developed more efficient mechanisms of locomotion. We thus hypothesize that the larvae choose paths through granular media that minimize their energy costs.

2 Methods

2.1 Model

We derived a simple model of energy cost for the larva that accounts for the frictional energy used to dig into a granular medium to a minimum depth h_0. The model assumes a constant angle of attack θ, which is defined as the angle below the horizontal at which the larva proceeds through the medium. It also assumes that the column of media above the larva is entirely supported by the shear and normal forces on its body, and that the larva's dorsal and ventral surfaces can be modeled as flat plates. Given θ, gravitational acceleration g, the product of the medium's density and packing factor ρ, the larva's width w, the length of the larva l_l, and the coefficient of sliding friction between the particles and larva μ_{pl}, the energy cost is expressed as the following:

$$E = \frac{w\rho g\mu_{pl}}{sin(2\theta) + \mu_{pl}}(h_0^2 l_l + l_l^2 sin(\theta) + \frac{l_l^3}{3}\sin^2(\theta)) \tag{1}$$

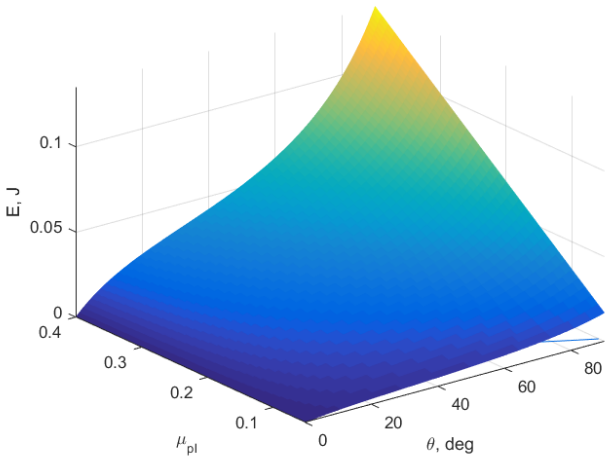

Figure 1: Graphical representation of Equation 1

The following expression gives the normal force on the larva's surface at a point located at a given depth h_i and with surface orientation θ_i relative to the horizontal:

$$\sigma_N = \frac{\rho g h_i}{\cos(\theta_i) + \frac{\mu_{pl}}{\sin(\theta_i)}} \tag{2}$$

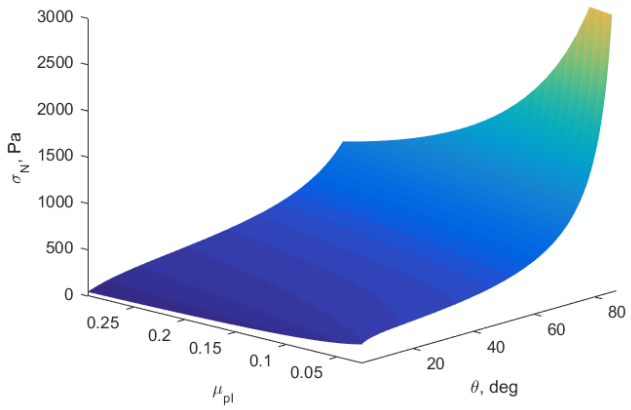

Figure 2: Graphical representation of Equation 2

Equation 1 and our hypothesis that the larvae will minimize their energy costs suggest that they will choose paths with low angles of attack, given the monotonic increase of E with both θ and μ_{pl}. Equation 2 similarly suggests that low angles of attack will be preferred, regardless of μ_{pl}, if the larvae attempt to stay under a normal stress threshold.

2.2 Setup

We constructed an acrylic test fixture with an adjustable divider in which to view the larvae. The divider, set 6mm away from the front plate, constrained the larvae to dig in only two dimensions to simplify analysis. Acrylic was chosen because it allowed the larvae to see be seen through the front and allowed the fixture to be lit from behind. Figure 3 shows the fixture design and Figure 4 shows the test setup. A Canon 60D with a EF-S 18-55mm f/3.5-5.6 IS lens was used for all videos. The larvae were filmed at 60fps with a resolution of 1280 x 720 pixels. We used the following granular media in our experiments: millet seeds, green mung seeds, black chia seeds, and glass beads.

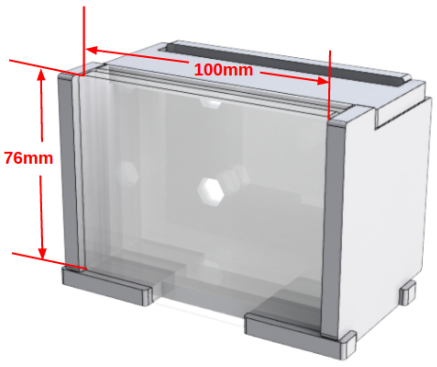

Figure 3: Rendering of test fixture CAD model

2.3 Frictional properties testing

To quantify the friction angle ψ, a measure of friction in granular media, we measured each medium's angle of repose. As shown in Figure 5, the angle of repose is the steepest angle that a conical pile of granular medium will support without sliding [8]. In granular media, the friction

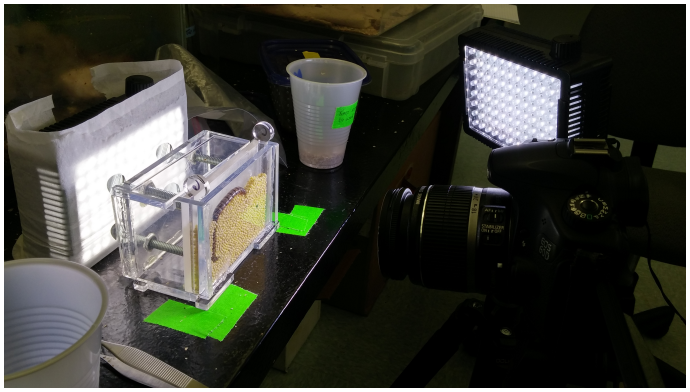

Figure 4: Photo of test setup

angle is equivalent to this angle of repose, and can be approximated by $\psi = \arctan \mu_{pp}$.

Figure 5: Illustration of angle of repose

We created piles of each medium, and measured each pile's height h and width w. We thus defined the friction angle as $\arctan\left(\frac{h}{\frac{w}{2}}\right)$, and the coefficient of static friction between particles as $\mu_{pp} = \frac{h}{\frac{w}{2}}$. Results are shown below in Table 1. The green mung and millet seeds fall close to the ranges of friction angle for bran and soil, and thus should be possible to dig within.

Table 1: Measurements of ψ and μ_{pp}. Those with N/A were taken from Pocket Ref [9]

Medium	μ_{pp}	ψ, deg
Glass beads	.13	14.6
Black chia seeds	.18	19.8
Green mung seeds	.26	27.5
Millet seeds	.32	32.6
Soil	N/A	30-45
Bran	N/A	30-45

2.4 Discrete Element Model

We will utilize a discrete element model (DEM) that simulates the interactions between particles and the larva in order to determine the forces exerted and energy expended by the larva. We will construct the DEM in the molecular dynamics software LAAMPS, and we will input the states of the larva and particles as recorded by the camera setup described in Section 2.2.

2.5 Tracking

In order to track the larvae, we placed markers on their segments after immobilizing them in a cold environment. These markers will be colored eyelash glue, in order to reduce toxicity and minimize the risk of influencing the larvae's behaviors.

We use image processing to track the movement of both the larvae and the granular media (see Appendix for complete code). To track the larvae, video frames are converted to the Hue Saturation Value (HSV) color space and were then filtered such that only regions with the hue, saturation, and value corresponding to our markers were left. This binary image is then segmented into regions, and holes are filled in. Our marker-tracking code then finds the centroid of each region as shown in Figure 6, which was tracked over the course of the video using an iterative closest point approach.

To track the the granular media, the frames are converted to the the HSV color space, again filtering out all areas not corresponding to the particles. Our code then employs morphological opening with a disc-shaped element to eliminate noise. A Hough circle transform finds the seeds and their centroids shown in Figure 7, and these centroids are then tracked frame by frame using an iterative closest point method.

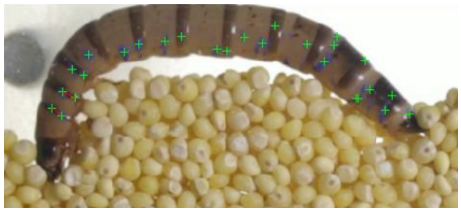

Figure 6: Larva with centroids of blue markers indicated in green

Figure 7: Centroids of millet seeds shown with black crosses

2.6 Preliminary Testing

In addition to creating image processing algorithms to collect key state variables of the system, we also conducted preliminary analysis manually to test our hypotheses. Larvae ($N = 3$) were each placed in each of the four media, and their movements recorded as described in Section 2.2. These videos were reviewed to find the frame at which the seventh-to-last segment of the larva's body entered the medium. At this frame, the angle of attack was calculated by manually identifying the centroid of the larva's head segment and the centroid of the dark band on the larva's seventh-to-last segment, and calculating the angle of the line between them.

3 Results

3.1 Preliminary Results

The larvae were able to dig to some degree in all of the four media that we tested, though they were not able to consistently and completely penetrate the glass beads or the green mung beans. Figure 8 shows the results of our preliminary angle of attack θ measurements versus the friction angle of the medium $\psi = \arctan \mu_{pp}$. There appears to be a linear relationship between ψ and θ: as the former increases, so does the latter. As shown in Table 2, however, the significance of this relationship $p = .2863$ is not strong enough to conclusively state that there is a relationship

between ψ and θ. It is apparent, though, that one outlier is the source of the lack of fit: for one of the trial runs in the millet seeds ($\psi = 32.6\,\text{deg}$), the larva dug at a much lower angle of attack than expected. Consulting the video, however, the larva only digs at that angle for a short time, then uses a much steeper angle.

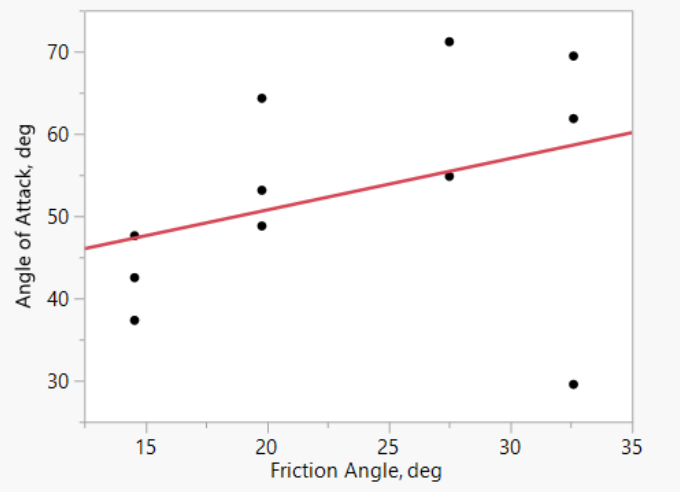

Figure 8: Scatter plot of angle of attack versus friction angle. Note outlier in the lower right-hand corner

Table 2: Results of ANOVA

Term	Estimate	Std Error	t Ratio	Prob>|t|
Intercept	38.186228	13.46223	2.84	0.0195*
Friction Angle, deg	0.6270184	0.55322	1.13	0.2863

To see how this outlier affects the data, we performed another ANOVA on the data with the outlier removed, shown below in Figure 9 and Table 3. The relationship in this case proves to be significant ($p < .01$).

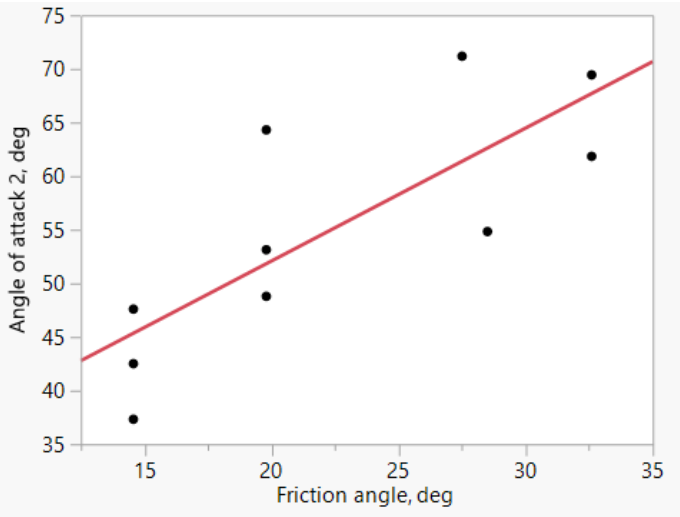

Figure 9: Scatter plot of angle of attack versus friction angle with outlier removed

Table 3: Results of second ANOVA

Intercept	27.286034	7.965522	3.43	0.0090*
Friction angle, deg	1.2398452	0.339435	3.65	0.0065*

3.2 Cavity formation and propagation

We noticed an unanticipated behavior while observing the larvae: the larvae formed a cavity as shown in Figure 10. This may relieve stress on the particles around the larva's head, allowing the larva to more easily move them. The larva then can use its head to move the media back towards its feet. With its feet the larvae pushes the media backwards while pushing its body forwards. While the larvae moves forward it continues forming this cavity below its head.

Figure 10: Cavity formed by larva

4 Discussion

The data and analysis presented in 3.1 suggest that there may be a relationship between frictional material properties and digging behavior, as expected. Contrary to the predictions of the model, though, the data suggest that rather than Equation 1 predicts, the larvae seem to prefer steeper angles, especially at higher values of μ_{pl}. This suggests that the model is either flawed or overly simplistic-there may, for example, be significant energy used in creating the cavities described in 3.2, or propagating them using the larva's legs. Another possibility, however, is that the larvae may simply not choose paths based on energy considerations or normal stress limitations.

The impact of the earlier-noted outlier on current data, however, suggests that more data are needed; currently, the sample size of 12 videos is too small to conclusively establish or disprove any relationship. Additionally, the methodology for collecting angle of attack data should be improved, since the data are highly dependent on what time in the video that they are collected and what the larva is doing at that moment. We also intend to make another observation chamber that is much larger and will allow us to take longer videos, investigate if the larva have a depth limit possibly based on normal stresses, and reduce the significance of particle-wall interactions.

The greatest limitation on our results is that we have yet to validate them with the results of the DEM. The DEM will be able to yield much greater insight into the forces and energy present, and how they may influence the larvae. Before we can construct it, though, we will need to more accurately measure properties such as μ_{pl} and refine our tracking algorithms to make them more consistent.

5 Conclusion

Preliminary results show that there may be a direct correlation between a medium's friction angle and the larva's angle of attack as it digs through it. More data is required to validate the significance this relationship, though.

We intend to gain further insight into the larvae's behavior with a discrete element model. To provide this model with inputs, we have created image processing algorithms that track both the larva and the surrounding granular medium particles.

References

[1] R. Godoy-Herrera, "Selection for digging behavior in drosophila melanogaster larvae," *Behavior genetics*, vol. 8, no. 5, p. 475, 1978.

[2] M. Isava and A. G. Winter V, "Razor clam-inspired burrowing in dry soil," *International Journal of Non-Linear Mechanics*, vol. 81, pp. 30–39, 2016.

[3] A. G. Winter, 5th, R. L. H. Deits, and A. E. Hosoi, "Localized fluidization burrowing mechanics of ensis directus," *The Journal of experimental biology*, vol. 215, no. Pt 12, p. 2072, 2012.

[4] R. D. Maladen, Y. Ding, C. Li, and D. I. Goldman, "Undulatory swimming in sand: Subsurface locomotion of the sandfish lizard," *Science*, vol. 325, no. 5938, pp. 314–318, 2009.

[5] Z. T. Self, A. J. Spence, and A. M. Wilson, "Speed and incline during thoroughbred horse racing: racehorse speed supports a metabolic power constraint to incline running but not to decline running," *Journal of Applied Physiology*, vol. 113, no. 4, pp. 602–607, 2012.

[6] A. Cohen, "Path preference of zophobas morio larvae during self-burial." December 2016.

[7] J. E. Niven and S. B. Laughlin, "Energy limitation as a selective pressure on the evolution of sensory systems," *The Journal of experimental biology*, vol. 211, no. Pt 11, pp. 1792–1804, 2008.

[8] Wikipedia, "Angle of repose — wikipedia, the free encyclopedia," 2016. [Online; accessed 13-December-2016].

[9] J. Baldwin, "Pocket ref," 1991.

List of Figures

List of Tables

A Code

A.1 Marker Tracker

```
%% Tracking markers on larva

%% clear and close all
%close all; clear;

%% Load video

% videoViewer allows for quick viewing of a video file
% Will only display grayscale video
vid = VideoReader('../Vids/vid1.mov');
warning('off', 'Images:initSize:adjustingMag');
k = 1;

%% main
while hasFrame(vid) && k < 101
    frame = readFrame(vid);
    frame = frame(20:580, 130:950,:);
    img_hsv = rgb2hsv(frame); % convert to hsv for better color tracking
%     img_hsv = img_hsv(20:580, 130:950,:); % crop unnecessary parts of image
    h = img_hsv(:,:,1);
    s = img_hsv(:,:,2);
    v = img_hsv(:,:,3);
    h_filt = h > .6 & h < .75;
    v_filt = v > .20;
    s_filt = s > .1;

    BW = h_filt & v_filt & s_filt;


    [B,L,N] = bwboundaries(BW,'noholes');

    % Calculate centroids for connected components in the image using regionprops.
    s = regionprops(L,'centroid');

    % Concatenate structure array containing centroids into a single matrix.
    centroids = cat(1, s.Centroid);

    %% distances
    length = centroids(1,1)-centroids(2,2);

    %% display
%     figure(1);
%     imshow(frame);

%     figure(2);
    %imshow(label2rgb(L, @jet, [.5 .5 .5]))
    imshow(frame)
    hold on
    plot(centroids(:,1),centroids(:,2), 'g+')
    line([centroids(1,1) centroids(2,1)], [centroids(1,2) centroids(2,2)], 'color',
    'r');
    line([centroids(3,1) centroids(5,1)], [centroids(3,2) centroids(5,2)], 'color',
    'r');
    hold off
    drawnow

    k = k + 1;
end


% img_cropped = img_raw(20:580, 130:950,:); % crop unnecessary parts of image
```

Code/video_marker_tracker.m

A.2 Media Tracker

```
% tests identification of granular media particles
% version 2016.11.10
% identifies the positions of granules over multiple frames
close all;

addpath('useful_code/mmread');

% video = mmread('C:\Users\Andy Cohen\Downloads\MVI_1555.MOV', [], [634 642]);
numFrames = length(video.times);
Times = video.times;
speedFactor = 1;

figure();
w = waitforbuttonpress;
if w == 0
    disp('Button click')
else
    disp('Key press')
end

for k = 1:10:numFrames
    img_raw = video.frames(k).cdata;
    img_cropped = img_raw(50:400, 535:985,:);

    [centers, radii] = findGranules(img_cropped);

%     circleMask = createCirclesMask(size(img_cropped(:,:,1)),centers,radii);
    imshow(img_cropped);
    set(gca,'position',[0 0 1 1],'units','normalized');
    hold on;
    plot(centers(:,1), centers(:, 2), '*k');
    title(sprintf('Time: %3g', Times(k)));
    hold off;
    pause(.001)



%     img_hsv = rgb2hsv(img_cropped);
%     h = img_hsv(:,:,1);
%     s = img_hsv(:,:,2);
%     v = img_hsv(:,:,3);
%     h_filt = h > .6 & h < .75;
%     v_filt = v > .20;
%     s_filt = s > .1;
%
%     overlay = h_filt & v_filt & s_filt;
%     hold on;
%     han = imshow(overlay);
%     set(han, 'AlphaData', .3*overlay);
end
```

Code/particle_segmenter_3.m

A.2.1 Find Granules

```
function [centers, radii] = findGranules(img_cropped)
    % finds granular media particles' positions in an image

    img_hsv = rgb2hsv(img_cropped);
    h = img_hsv(:,:,1);
    s = img_hsv(:,:,2);
    v = img_hsv(:,:,3);
    h_filt = h > .09 & h < .15;
    v_filt = v > .4;
    s_filt = s < .6;

    overlay = h_filt & v_filt & s_filt;
    overlay = imopen(overlay, strel('disk', 5));
    img_gray = double(rgb2gray(img_cropped));
    overlay_2 = double(overlay);
    img_overlaid = uint8(overlay_2.*img_gray);

    addpath('useful_code/circleFinder');
    [centers, radii] = imfindcircles(img_overlaid, [6 15], ...
        'Sensitivity', 0.9371, ...
        'EdgeThreshold', 0.22, ...
        'Method', 'PhaseCode', ...
        'ObjectPolarity', 'Bright');
end
```

Code/findGranules.m